STATIC AND DYNAMIC ANALYSIS OF FUNCTIONALLY GRADED FLAT PANELS

A THESIS SUBMITTED IN PARTIAL FULFILLMENT OF

THE REQUIREMENTS FOR THE DEGREE OF

Bachelor of Technology

In

Mechanical Engineering

By

Bikash Kumar Majhi

Roll No.:109ME0159

DEPARTMENT OF MECHANICAL ENGINEERING

NATIONAL INSTITUTE OF TECHNOLOGY

ROURKELA-769008

MAY 2013

STATIC AND DYNAMIC ANALYSIS OF FUNCTIONALLY GRADED FLAT PANELS

A THESIS SUBMITTED IN PARTIAL FULFILLMENT OF

THE REQUIREMENTS FOR THE DEGREE OF

Bachelor of Technology

In

Mechanical Engineering

By

Bikash Kumar Majhi

Roll No.:109ME0159

Under the guidance of

Prof. S. K. Panda

DEPARTMENT OF MECHANICAL ENGINEERING

NATIONAL INSTITUTE OF TECHNOLOGY

ROURKELA-769008

MAY 2013

NATIONAL INSTITUTE OF TECHNOLOGY

ROURKELA

CERTIFICATE

This is to certify that the work in this thesis entitled "***Static and Dynamic analysis of Functionally Graded Flat Panels***" by ***Bikash Kumar Majhi***, roll no ***109ME0159*** has been carried out under my supervision in partial fulfilment of the requirements for the degree of *Bachelor of Technology in Mechanical Engineering* during session 2012-2013 in the *Department of Mechanical Engineering, National Institute of Technology, Rourkela*.

To the best of my knowledge, this work has not been submitted to any other University/Institute for the award of any degree or diploma.

Dr. Subrata Kumar Panda

(Supervisor)
Assistant Professor
Department of Mechanical Engineering
National Institute of Technology, Rourkela

Date: 08/05/2013

ACKNOWLEDGEMENT

I wish to express my sincere gratitude to **Dr. Subrata Kumar Panda** for his inspiring encouragement, guidance and efforts taken throughout the entire course of this work. His constructive criticism, timely help, and efforts made it possible to present the work contained in this Thesis.

I am grateful to Prof. S.K. Sarangi, Director, and Prof K.P Maity, Head of the Department, Mechanical Engineering, for their active interest and support.

I would like to thank **Mr. Girish Kumar Sahu, M.Tech** and **Mr. Pankaj Katariya, M.Tech (Res)** , Department of Mechanical Engineering, National Institute of Technology, Rourkela for their constant help in understanding of the technical aspects of the project. I will also be grateful to **Ph.D scholar Mr. Vishesh Ranjan Kar,** for his constant help in the successfully carrying out the new results.

I express my deep sense of gratitude and reverence to my beloved parents for their blessings, patience and endeavour to keep my moral high at all times. Last but not the least, I wish to express my sincere thanks to all those who directly or indirectly helped me at various stages of this work.

Bikash Kumar Majhi

109ME0159

CONTENTS

			Pages
1.	**INTRODUCTION**		**1-3**
	1.1	Background	2
	1.2	Application of FGM	3
	1.3	Objective of the work	3
2.	**LITERATURE REVIEW**		**4-7**
	2.1	Static analysis	5
	2.2	Dynamic analysis	6
3.	**FINITE ELEMENT FORMULATION**		**8-12**
4.	**EFFECTIVE MATERIAL PROPERTY**		**13-16**
	4.1	Exponential law	14
	4.2	Power law	14
	4.3	FE modelling of FGM plates	16
5.	**STATIC ANALYSIS**		**17-26**
	5.1	FG model (ANSYS)	18
	5.2	Convergence and validation	18
	5.3	Numerical results	19
		5.3.1 Aluminium/Zirconia plate	20
		5.3.2 Different boundary conditions	21
		5.3.3 Aluminium/Alumina plate	23
		5.3.4 Silicon Nitride/Stainless steel plate	25
6.	**DYNAMIC ANALYSIS**		**27**
	6.1	FG model (ANSYS)	28
	6.2	Numerical results	28
7.	**CONCLUSION**		**31**
	7.1	Conclusion	32
	7.2	Future scope of work	32
8.	**REFERENCE**		**33**
9.	**APPENDIX-A**		**36**

ABSTRACT

Functionally graded materials have received a lot of interest in recent days by their diversified and potential applications in aerospace and other industries. They have high specific mechanical properties and high temperature capabilities which makes them special over all the exiting advanced materials. The present work investigated static and dynamic analysis of functionally graded plate. The material properties vary continuously from metal (bottom surface) to ceramic (top surface). The effective material properties of functionally graded materials for the plate structures are assumed to be temperature independent and graded in the plate thickness direction according to a power law distribution of the volume fractions of the constituents. The present model is developed using ANSYS parametric design language code in the ANSYS platform. An eight noded isoparametric quadrilateral shell element is used to discretise the present model for both static as well as dynamic analysis. A convergence test has been done with different mesh refinement and compared with published results. The parametric study indicates that the power-law indices, thickness ratios, aspect ratios, support conditions and different material properties have significant effect on non-dimensional mid-point deflection.

LIST OF FIGURES

Figure No		Pages
Figure 1	Geometry and dimensions of the FG plate	9
Figure 2	Variations of volume fraction of ceramic through non-dimensional thickness coordinate	15
Figure 3	Variations of volume fraction of metal through non-dimensional thickness coordinate	15
Figure 4	FGM plate modelled in ANSYS 13.0 using SHELL281 element	16
	Convergence study	
Figure 5	Variation of non-dimensional mid-point deflection with different mesh size in ANSYS SHELL 181 model for simply supported FGM plate	19
	Static analysis of Aluminum/Zirconia plate	
Figure 6	Variation of non-dimensional mid-point deflection with different mesh size in ANSYS SHELL 181 model for simply supported FGM plate	20
Figure 7	Variation of non-dimensional mid-point deflection with different thickness ratio (a/h ratio) in ANSYS SHELL 281 model for simply supported FGM plate	20
Figure 8	Variation of non-dimensional mid-point deflection with different aspect ratio (a/b ratio) in ANSYS SHELL 281 model for simply supported FGM plate	21
	Different boundary conditions	
Figure 9	Non-dimensional deflection vs. Length to thickness ratio square FGM plate with simply supported (SSSS) boundary condition	21
Figure 10	Non-dimensional deflection vs. Length to thickness ratio square FGM plate with clamped (CCCC) boundary condition	22
Figure 11	Non-dimensional deflection vs. Length to thickness ratio square FGM plate with clamped-simply supported (CSCS) boundary condition	22
Figure 12	Non-dimensional deflection vs. Length to thickness ratio square FGM plate with clamped-simply supported (SSCC) boundary condition	23
	Aluminum/Alumina plate	
Figure 13	Variation of non-dimensional mid-point deflection with different mesh size in ANSYS SHELL 281 model for simply supported FGM plate	23
Figure 14	Variation of non-dimensional mid-point deflection with different thickness ratio (a/h ratio) in ANSYS SHELL 281 model for simply supported FGM plate	24

LIST OF FIGURES

Figure No		Pages
Figure 15	Variation of non-dimensional mid-point deflection with different aspect ratio (a/b ratio) in ANSYS SHELL 281 model for simply supported FGM plate	24
	Silicon Nitride/Stainless steel plate	
Figure 16	Variation of non-dimensional mid-point deflection with different mesh size in ANSYS SHELL 281 model for simply supported FGM plate	25
Figure 17	Variation of non-dimensional mid-point deflection with different thickness ratio (a/h ratio) in ANSYS SHELL 281 model for simply supported FGM plate	25
Figure 18	Variation of non-dimensional mid-point deflection with different aspect ratio (a/b ratio) in ANSYS SHELL 281 model for simply supported FGM plate	26
	Dynamic analysis of Aluminum/Zirconia plate	
Figure 19	Deflection of mid-point of simply supported FG flat panel with n=0	28
Figure 20	Deflection of mid-point of simply supported FG flat panel with n=1	29
Figure 21	Deflection of mid-point of simply supported FG flat panel with n=2	29
Figure 22	Deflection of mid-point of simply supported FG flat panel with n= ∞	30
Figure 23	Deflection of mid-point of simply supported FG flat panel with n=0 in time interval of 0.0001 to 0.012s	30

LIST OF TABLES

Table No		Pages
Table 1	Properties of the FGM plate constituents	16
Table 2	Convergence study of non-dimensional mid-point deflection of simply supported FG (Al_2O_3/ZrO_2) flat panel with $a/b = 1$ and $a/h = 5$)	19

NOMENCLATURE

a	Length of plate
b	Width of plate
h	Height of plate
a/h	Thickness ratio
a/b	Aspect ratio
u, v, w	Displacement field in x, y, z direction
u^0, v^0, w^0	Mid-plane displacement in x, y, z direction
$\theta_x, \theta_y, \theta_z$	Rotational displacement in x, y, z direction
$\varepsilon_{xx}, \varepsilon_{xy}, \varepsilon_{xz}$	Lateral strain
$\gamma_{xz}, \gamma_{xy}, \gamma_{yz}$	Shear strain
R_x, R_y, R_z	Radius of curvature in x, y, z direction
$E(z)$	Young's modulus of material
υ	Poisson's ratio
δ	Displacement vector
ε	Strain vector
[B]	Strain-displacement matrix
[D]	Rigidity matrix
[K]	Stiffness matrix
[M]	Mass matrix
J	Jacobian matrix
$F(t)$	Time-dependent force
E_c	Young's modulus of ceramic
E_m	Young's modulus of metal
ρ_c	Density of ceramic
ρ_m	Density of metal
υ_c	Poisson's ratio of ceramic
υ_m	Poisson's ratio of ceramic

Chapter I

Introduction

CHAPTER-1 INTRODUCTION

1.1 Background

Laminated composites have received a lot of interest in recent days by diversified and potential applications in automotive and aerospace industry due to their strength to weight, stiffness to weight ratio, low fatigue life and toughness and other higher material properties. These are made from two or more constituent materials which have different chemical or physical properties and produced a material having different behaviour from the individual. These are used in buildings, storage tanks, bridges etc. Each layer is laminated in order to get superior material properties. The individual layer has high strength fibres like graphite, glass or silicon carbide and matrix materials like epoxies, polyimides. By varying the thickness of laminas desired properties (strength, wear resistance, stiffness) can be achieved.

Although these materials have superior properties, their major drawback is the weakness of laminated materials. This is known as delamination phenomenon which leads to the failure of the composite structure. Residual stresses are present due to difference in thermal expansion of the matrix and fibre. It is well known that at high temperature the adhesive being chemically unstable and fails to hold the lamination. Sometimes due to fibre breakdown it also prematurely fails.

Functionally Graded Material (FGM) is combination of a ceramic and a metal. A material in which its structure and composition both varies gradually over volume in order to get certain specific properties of the material hence can perform certain functions. The properties of material depend on the spatial position in the structure of material. The effect of inter-laminar stress developed at the laminated composite interfaces due to sudden change of material properties reduced by continuous grading of material properties. Generally microstructural heterogeneity or non-uniformity is introduced in functionally graded material. The main purpose is to increase fracture toughness, increase in strength because ceramics only are brittle in nature. Brittleness is a great disadvantage for any structural application. These are manufactured by combining both metals and ceramics for use in high temperature applications. Material properties are varies smoothly and continuously in one or many directions so FGMs are inhomogeneous. FGM serves as a thermal barrier capable of withstanding 2000K surface temperature. Fabrication of FGM can be done by different processing such as layer processing, melt processing, particulate processing etc. FGM has the ability to control shear deformation, corrosion, wear, buckling etc. and also to remove stress

concentrations. This can be used safely at high temperature also as furnace liners and thermal shielding element in microelectronics and thermal protection systems for spacecraft, hypersonic and supersonic planes and in combustion chamber also.

1.2 Application of FGM

i. Engineering Application
    a. Shafts
    b. Engine parts
    c. Blades of turbine
ii. Aerospace Engineering
    a. Rocket engine components
    b. Aerospace parts and skins
iii. Electronics
    a. Sensor
    b. Actuator
    c. Integrated chips
    d. Semiconductor
iv. Biomaterials
    a. Artificial bones
    b. Drug delivery system

1.3 Objective of the work

The objective of the present study is to analyse the static and dynamic behaviour of FG flat panel under different volume fraction indices, aspect ratios, thickness ratios and different support conditions. ANSYS parametric design language (APDL) code is use to develop the model in ANSYS13.0 platform and solve the problem using appropriate algorithm. The present model is discretised by using an eight noded isoparametric quadrilateral shell element (SHELL281), as defined in the ANSYS element library. Three types of FG flat panels are used in this study namely, Aluminium/Alumina, Aluminium/Zirconia and Silicon Nitride/Stainless steel. The effects of different parameters on non-dimensional mid-point deflection are studied.

Chapter II

Literature review

FG material plates have created revolution in aerospace industry for its thermal properties, multifunctionalities. It also provides opportunities to take the benefits of different material system. Its static and dynamic analysis is necessary to estimate the properties of flat panels. Many researchers reported static and dynamic behaviour of functionally graded plates based on different theories and developed new methods of solutions.

2.1 Static and vibration analysis

Talha and Singh [1] investigated the free vibration and static analysis of rectangular FGM plates using higher order shear deformation theory with a special modification in the transverse displacement in conjunction with finite element models. Neves et *al.* [2] studied the static deformations analysis of functionally graded plates by collocation with radial basis functions, according to a sinusoidal shear deformation formulation for plates. Aragh and Hedayati [3] studied the characteristics of free vibration and static response of a 2-D FGM open cylindrical shell. Formulations are done by 2-D generalized differential quadrature method (GDQM). Ferreira *et al*. [4] studied static deformations of functionally graded square plates of different aspect ratios using meshless collocation method, the multiquadric radial basis functions and a third-order shear deformation theory. Reddy[5] studied static and dynamic analysis of FGM plates using third-order shear deformation theory. Navier solutions are obtained for a simply supported square plate. Abrate[6] investigated static, buckling and free vibration deflections of FGM plates by using classical plate theory, FSDT model and HSDT model. Zenkour[7] studied the static behaviour of a rectangular FG plate under simply supported condition and subjected to uniform transverse load. Ferreira *et al.* [8] studied static deformations of simply supported functionally graded plate by using HSDT and multiquadric radial basis functions. Vel and Batra[9] investigated the exact 3-D elasticity solutions of simply supported rectangular FG plates under thermo-mechanical load. The author has assumed power law for material volume fractions. The exact solutions of displacements and stresses are used to find out the accuracy of the solutions. Qian *et al.*[10] investigated plain strain static thermostatic deformations of simply supported thick rectangular FG elastic plate. Displacement and stress are computed and validated from the 3D exact solutions of the problem. Ramirez *et al.*[11] studied static analysis of 3D, elastic, anisotropic FG plates. The

author has taken simply supported graphite/epoxy material for analysis. Zenkour [12] further studied the static response of FG plates using shear deformation plate theory using power law for grading. Bhangale and Ganesan[13] investigated static analysis of simply supported FG plates which are exponentially graded in the thickness direction. Aghdam *et al.*[14] studied static analysis foe bending of FG clamped thick plates. The solutions are compared with the solutions of finite element code ANSYS, power law is used for grading the properties in thickness direction. Neves *et al.*[15] investigated the static deformations of FG square plates using radial basis function. Talha and Singh [16] investigated the static and free vibration analysis using C^0 finite element with 13 degrees of freedom per node and formulated by HSDT. Nguyen-Xuan *et al.*[17] studied the static, free vibration and mechanical/thermal buckling problems of FG plates by Reisnner/Mindlin plate theory.

2.2 Dynamic Analysis

Yang and Shen [18] studied dynamic response of FGM thin plates under initial stress and partially distributed impulsive lateral loads. The author used silicon nitride/ stainless steel rectangular plates, assumed temperature dependent material properties clamped on two opposite edges, used power law for grading and used Modal superposition method for transient response. In 2001 Yang and Shen [19] studied free and forced vibration analysis for the same plate and found functionally graded plate with material properties intermediate to isotropic material do not necessarily have intermediate natural frequency if thermal effects are considered. Liew *et al.* [20] investigated dynamic stability of symmetrically laminated FGM rectangular plates under uniaxial plane load. Formulation is done by Reddy's third-order shear deformation theory and material is silicon nitride and stainless steel. [21]Kim studied vibration characteristics of rectangular FGM plate under initial stress. Third-order shear deformation plate theory is adopted and Rayleigh-Ritz procedure is applied for getting frequency equation. Lanhe *et al.* [22] investigated dynamic stability of thick FGM plate under aero-thermo-mechanical loads and used novel numerical solution technique. The equations for dynamic analysis are derived by Hamilton's principle. For different parameters dynamic instability regions are studied. Ansari and Darvizeh [23] investigated vibrational behaviour of functionally graded shells, based on first-order shear deformation shell theory. The grading functions are power law, sigmoid and exponential distribution. Behjat *et al.* [24] studied dynamic response, static bending of functionally graded piezoelectric material plate (PZT-4/PZT-5H), formulated by using potential energy and Hamilton's principle. Effects of material composition and boundary conditions on dynamic response are also studied. Sladek

et al. [25] investigated dynamic analysis of FG plates by MPLG method. For displacement field author used Reissner-Mindlin plate bending theory. Simply supported and clamped boundary conditions are taken in to consideration. Wen *et al.* [26] studied 3-D analysis of isotropic and orthotropic FG plates with simply supported edge under dynamic loads. The equations formulated is based on state-space approach in Laplace transform domain and solved by RBF method. Grading has done by exponential method as well as volume fraction law. Shariyat [27] studied the vibration and dynamic buckling response of rectangular FG plates under thermo-mechanical loading. A nine noded second-order formulation has done and graphs are studied under temperature dependent material properties.

From the above study it has been seen that very few researcher studied the dynamic analysis of FG plates. Since most of the practical cases deals with transient or dynamic load, its responses has to be analysed with different parameters like volume fraction index. This work analysed dynamic responses of aluminium/zirconia flat panel under step load with different volume fraction index (n=0, 1, 2, ∞);

Chapter III

Finite element formulation

In the present analysis, a FG plate of uniform thickness *h* with rectangular base of sides *a* and *b* is established through APDL code and shown in the Figure 1. The FG plate model is developed in ANSYS based on the inbuilt FSDT kinematics. The displacements field u, *v* and *w* at any point along *x*, *y* and *z* axes can be written as follows:

$$\begin{aligned} u(x,y,z) &= u^0(x,y) + z\theta_x(x,y) \\ v(x,y,z) &= v^0(x,y) + z\theta_y(x,y) \\ w(x,y,z) &= w^0(x,y) + z\theta_z(x,y) \end{aligned} \tag{1}$$

where, *u*, *v* and *w* denote displacements; u^0, v^0 and w^0 are the mid-plane displacements in x, y, z axes respectively and θ_x, θ_y and θ_z are the shear rotations.

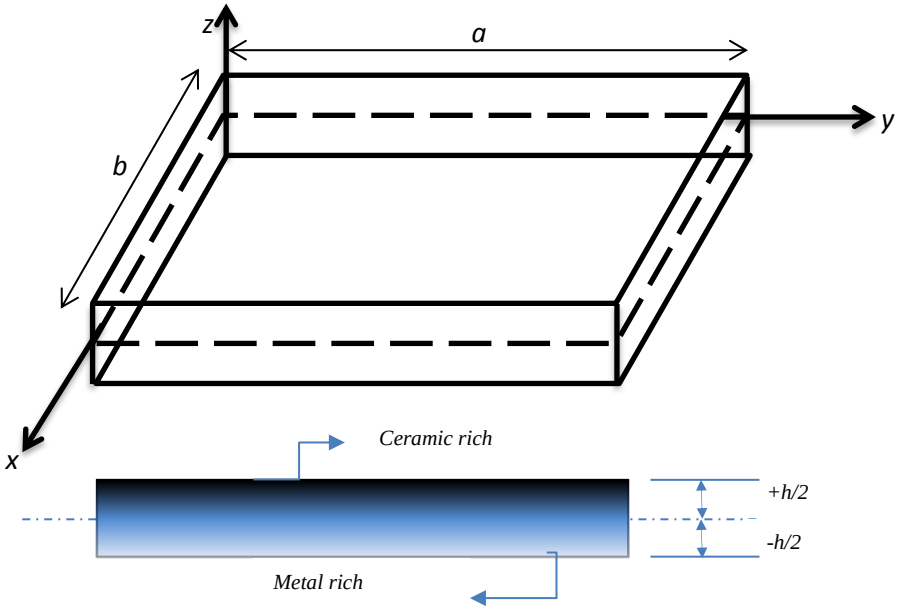

Figure 1: Geometry and dimensions of the FG plate

The linear stains corresponding to the displacement field is

$$\begin{aligned} \varepsilon_{xx} &= \frac{\partial u}{\partial x} + \frac{w}{R_x}, & \gamma_{yz} &= \theta_y + \frac{\partial w}{\partial y} - \frac{v}{R_y}, \\ \varepsilon_{yy} &= \frac{\partial v}{\partial y} + \frac{w}{R_y}, & \gamma_{xz} &= \theta_x + \frac{\partial w}{\partial y} - \frac{u}{R_x}, \\ \varepsilon_{zz} &= \theta_z, & \gamma_{xy} &= \frac{\partial u}{\partial y} + \frac{\partial v}{\partial x} + \frac{2w}{R_{xy}} \end{aligned} \tag{2}$$

For the flat panel i.e. plate, $R_x = R_y = R_{xy} = \infty$

It can be rewritten as

$$\left\{\bar{\varepsilon}\right\} = \left\{\varepsilon_{xx}, \varepsilon_{yy}, \varepsilon_{zz}, \gamma_{yz}, \gamma_{xz}, \gamma_{xy}\right\}^T, \tag{3}$$

$$\varepsilon_{l} = \begin{bmatrix} \varepsilon_{xx} \\ \varepsilon_{yy} \\ \varepsilon_{zz} \\ \gamma_{yz} \\ \gamma_{xz} \\ \gamma_{xy} \end{bmatrix} = \begin{bmatrix} \varepsilon_{x}^{0} \\ \varepsilon_{y}^{0} \\ \varepsilon_{z}^{0} \\ \varepsilon_{yz}^{0} \\ \varepsilon_{xz}^{0} \\ \varepsilon_{xy}^{0} \end{bmatrix} + z \begin{bmatrix} k_{x}^{'} \\ k_{y}^{'} \\ k_{z}^{'} \\ k_{yz}^{'} \\ k_{xz}^{'} \\ k_{xy}^{'} \end{bmatrix} \tag{4}$$

where $\varepsilon_x^0 = \frac{\partial u^0}{\partial x} + \frac{w^0}{R_x}$, $\varepsilon_y^0 = \frac{\partial v^0}{\partial y} + \frac{w^0}{R_y}$, $\varepsilon_z = 0$, $\varepsilon_{yz}^0 = \theta_y + \frac{\partial w^0}{\partial y} - \frac{v^0}{R_y}$, $\varepsilon_{xz}^0 = \theta_x + \frac{\partial w^0}{\partial y} - \frac{u^0}{R_x}$,

$\varepsilon_{xy}^0 = \frac{\partial u^0}{\partial y} + \frac{\partial v^0}{\partial x} + \frac{2w^0}{R_{xy}}$, $k_x^{'} = \frac{\partial \theta_x}{\partial x} + \frac{\theta_z}{R_x}$, $k_y^{'} = \frac{\partial \theta_y}{\partial y} + \frac{\theta_z}{R_y}$, $k_y^{'} = \theta_z$, $k_{yz}^{'} = \frac{\partial \theta_z}{\partial y} + \frac{\theta_y}{R_y}$,

$k_{xz}^{'} = \frac{\partial \theta_z}{\partial y} + \frac{\theta_x}{R_x}$, $k_{xy}^{'} = \frac{\partial \theta_x}{\partial y} + \frac{\partial \theta_y}{\partial x} + \frac{\theta_z}{R_{xy}}$

The linear constitutive relations are

$$\begin{Bmatrix} \alpha_{xx} \\ \alpha_{yy} \\ \alpha_{zz} \\ \alpha_{yz} \\ \alpha_{xz} \\ \alpha_{xy} \end{Bmatrix} = \begin{bmatrix} Q_{11} & Q_{12} & Q_{13} & 0 & 0 & 0 \\ Q_{21} & Q_{22} & Q_{23} & 0 & 0 & 0 \\ Q_{31} & Q_{32} & Q_{33} & 0 & 0 & 0 \\ 0 & 0 & 0 & Q_{44} & 0 & 0 \\ 0 & 0 & 0 & 0 & Q_{55} & 0 \\ 0 & 0 & 0 & 0 & 0 & Q_{66} \end{bmatrix} \begin{Bmatrix} \varepsilon_{xx} \\ \varepsilon_{yy} \\ \varepsilon_{zz} \\ \gamma_{yz} \\ \gamma_{xz} \\ \gamma_{xy} \end{Bmatrix} \tag{5}$$

where,

$$Q_{11} = Q_{12} = Q_{13} = \frac{E(z)(1-\nu^2)}{(1-3\nu^2-2\nu^3)}$$

$$Q_{12} = Q_{13} = Q_{23} = \frac{E(z)\nu(1+\nu)}{(1-3\nu^2-2\nu^3)}$$

$$Q_{44} = Q_{55} = Q_{66} = \frac{E(z)}{2(1+\nu)}$$

The modulus of elasticity *E(z)* and elastic coefficients Q_{ij} vary through the plate thickness.

For the implementation of finite element method, the developed model is discretised by using an eight noded isoperimetric quadrilateral shell element (SHELL281), as defined in the ANSYS element library. This element is suitable for analysing thin to moderately-thick shell structures with six degrees of freedom.(three translations and three rotations) at each

node in the *x*, *y* and *z* directions. The displacements are expressed in terms of interpolation functions (N_i)

$$\delta = \sum_{i=1}^{8} N_i \delta_i \tag{6}$$

where, $\delta_i = \left[u^0, v^0, w^0, \theta_x, \theta_y, \theta_z\right]^T$. The interpolation functions for eight noded isoperimetric quadrilateral shell element in natural (ξ-η) coordinates are given as [15]

$$N_1 = \frac{1}{4}(1-\xi)(1-\eta)(-\xi-\eta-1)\ , \qquad N_2 = \frac{1}{4}(1+\xi)(1-\eta)(\xi-\eta-1),$$

$$N_3 = \frac{1}{4}(1+\xi)(1+\eta)(\xi+\eta-1), \qquad N_4 = \frac{1}{4}(1-\xi)(1+\eta)(-\xi+\eta-1),$$

$$N_5 = \frac{1}{2}(1-\xi^2)(1-\eta), \qquad N_6 = \frac{1}{2}\left(1+\xi\right)\left(1-\eta^2\right),$$

$$N_7 = \frac{1}{2}\left(1-\xi^2\right)\left(1+\eta\right), \qquad N_8 = \frac{1}{2}\left(1-\xi\right)\left(1-\eta^2\right) \tag{7}$$

The strain vector in terms of nodal displacement vector can be written as

$$\{\varepsilon\} = [B]\{\delta\} \tag{8}$$

where, $[B]$ is the strain-displacement matrix containing interpolation functions and derivative operators and $\{\delta\}$ is the nodal displacement vector.

The generalized stress-strain relation with respect to its reference plane can be written as

$$\{\sigma\} = [D]\{\varepsilon\} \tag{9}$$

where $\{\sigma\} = \left\{\sigma_x \quad \sigma_y \quad \sigma_z \quad \tau_{xy} \quad \tau_{yz} \quad \tau_{xz}\right\}^T$ and $\{\varepsilon\} = \left\{\varepsilon_x \quad \varepsilon_y \quad \varepsilon_z \quad \gamma_{xy} \quad \gamma_{yz} \quad \gamma_{xz}\right\}^T$ are the linear stress and strain vector, respectively and $[D]$ is the rigidity matrix.

$$[\overline{Q}] = [T]^T [Q][T] \tag{10}$$

$$[D] = \int_{-h/2}^{h/2} [\overline{Q}] dz \tag{11}$$

The elemental stiffness matrix $[K]^e$ and the mass matrix $[M]^e$ are integrated by using Gauss-quadrature integration over the domain to obtain the global stiffness and mass matrices and this can be conceded as

$$[K]^e = \int_{-1}^{+1}\int_{-1}^{+1} [B]^T [D][B]|J| d\xi d\eta \tag{12}$$

$$[M]^e = \int_{-1}^{+1}\int_{-1}^{+1} [N]^T [m][N]|J| d\xi d\eta \tag{13}$$

where, $|J|$ is the determinant of the Jacobian matrix and [*N*] is the interpolation function matrix. The jacobian is used to map the domain from natural coordinate to the general coordinate.

The governing equation of static analysis of FG plate under force *F* can be expressed as follows:

$$[K]\{\delta\} - \{F\} = 0 \tag{14}$$

where, [K] is the global stiffness matrices. Eqn. (8) is a generalized eigenvalue problem and non-dimensional central point deflection can be found from this equation.

The governing equation of dynamic analysis of FG plate under dynamic load *F (t)* can be expressed as follows:

$$[K]\{\delta\} + [M]\{\ddot{\delta}\} = \{F(t)\} \tag{15}$$

Chapter IV

Effective material properties

The effective material properties of the FGM plate are assumed to be varying continuously along their thickness direction as discussed earlier and are obtained by using a simple power-law distribution or exponential law which counts the volume fraction of each constituent.

4.1 Exponential law

Exponential law of grading FGM states that for a FGM structure of uniform thickness '*h*', the material properties '*P(z)'* at any point located at '*z*' distance from the mid-plane surface is given by:

$$P(z) = P_t e^{\left(-\lambda\left(1-\frac{2z}{h}\right)\right)} \text{ , where, } \quad \lambda = \frac{1}{2}\ln\left(\frac{P_t}{P_b}\right) \tag{16}$$

$P(z)$ denotes material property like Young's modulus of elasticity (*E*), shear modulus of elasticity (*G*), Poisson's ratio (υ), material density (ρ) of the FGM structure. P_t and P_b are the material properties at the top (*z=+h/2*) and bottom (*z=-h/2*) surfaces. λ is the material grading indexes which depend on the design requirements.

4.2 Power law

The power-law distribution of a panel considered from the mid-plane reference plane can be written as

$$V_f = \left(\frac{z}{h}+\frac{1}{2}\right)^n \tag{17}$$

where, *n* is the power-law index, $0 \le n \le \infty$. The variations of volume fraction of the ceramic and metal phase through the non-dimensional thickness coordinate are plotted in Figure 2 and 3 for five different values of power-law indices (n = 0.2, 0.5, 1, 2 and 10). The functionally graded material with two constituents and their properties such as, Young's modulus *E* and the mass density ρ have been obtained using the following steps.

$$E = \left(E_c - E_m\right)\left(\frac{z}{h}+\frac{1}{2}\right)^n + E_m \tag{18}$$

$$\rho = \left(\rho_c - \rho_m\right)\left(\frac{z}{h}+\frac{1}{2}\right)^n + \rho_m \tag{19}$$

$$\upsilon = \left(\upsilon_c - \upsilon_m\right)\left(\frac{z}{h}+\frac{1}{2}\right)^n + \upsilon_m \tag{20}$$

In the present work, the power- law distribution is used for the continuous gradation of material properties in thickness direction.

The effective material properties are calculated based on the Eqns. (18), (19) and (20), when $z = - h/2$, $E = E_m$, $\rho = \rho_m$ and $\upsilon = \upsilon_m$ similarly, when $z = + h/2$; $E = E_c$, $\rho = \rho_c$ and $\upsilon = \upsilon_c$ i.e., the material properties vary continuously from metal at the bottom surface to ceramic at the top surface. The Poisson's ratio ν is assumed to be constant throughout the thickness of the shell panel. The properties of the FGM constituents at room temperature (27^oC) are used for the analysis and presented in Table 1. The different material properties are used to analyse the responses for throughout the study.

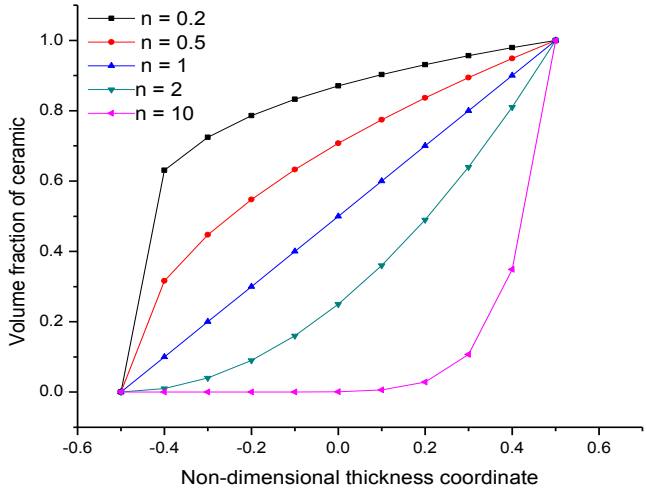

Figure 2: Variations of volume fraction of ceramic through non-dimensional thickness coordinate

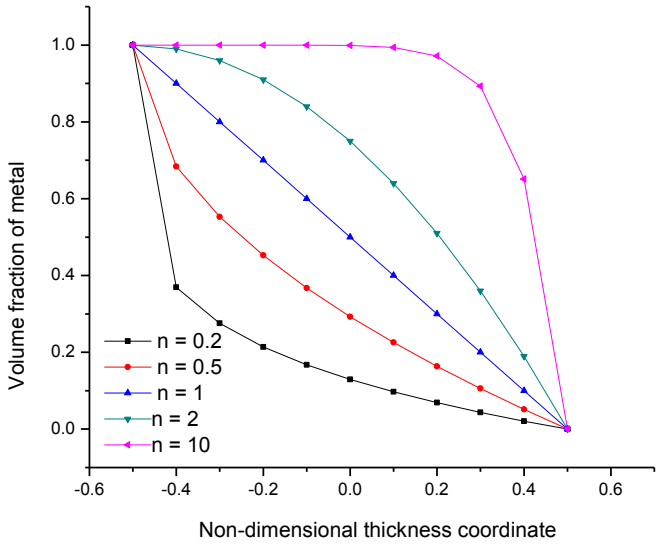

Figure 3 Variations of volume fraction of metal through non-dimensional thickness coordinate

Table 1: Properties of the FGM plate constituents

Materials	*Properties*		
	Young's Modulus E (GPa)	*Poisson's Ratio* ϑ	*Density* (Kg/m^3) ρ
Aluminium (Al)	*70*	*0.3*	*2707*
Alumina (Al_2O_3)	*380*	*0.3*	*3800*
Zirconia (ZrO_2)	*151*	*0.3*	*3000*
Silicon Nitride (Si_3N_4)	*348.43*	*0.28*	*2370*
Steel (SUS304)	*201.04*	*0.28*	*8166*

4.3 FE Modelling of FGM plates:

FGM plates with different length to thickness ratio(a/h) , aspect ratio (a/b) are analysed in this experiment. The analysis is performed in commercially available software (ANSYS 13.0). The loading conditions are assumed to be static. The element chosen for this analysis is SHELL281, which is a layered version of the 8-node structural shell model. This is suitable for analysing thin to moderately-thick shell structures. This shell element has six degrees of freedom at each node namely three translations and three rotation in the nodal x, y and z directions respectively. The FGM plate is modelled in ANSYS 13.0 as shown in the fig 4.

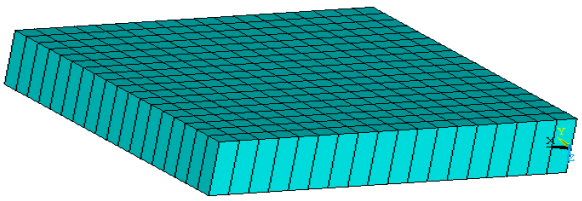

Figure 4: FGM plate modelled in ANSYS 13.0 using SHELL281 element

Chapter V

Static analysis

5.1 FG model (ANSYS)

The static responses of the FG plates are analysed using ANSYS 13.0 under static surface load for simply supported boundary condition for Aluminium/Zirconia FG flat panel. The computed results are validated and compared with those available in the literature. The analysis is carried out for thickness ratio (a/h) = 5, aspect ratio (a/b=1) with different volume fraction indices. APDL code has been developed in ANSYS 13.0 for analysing the above panel. The following non-dimensional parameters are used:

Central deflection $\bar{w} = \frac{w}{h}$

Load parameter $P_o = \frac{P}{E_2 h^4}$ (21)

5.2 Convergence and validation:

The static analysis of FG plates is analysed by ANSYS 13.0 using APDL program. The aluminium/zirconia material is analysed for different mesh size under simply supported boundary condition. These boundary conditions are there to reduce the no of unknowns from the final equation and in order to avoid rigid body motion.

Simply-supported (SSSS): $v^0 = w^0 = \theta_y = \theta_z = 0$ at $x=0$ and a

$u^0 = w^0 = \theta_x = \theta_z = 0$ at $y = 0$ and b

For validation of obtained data and the efficiency of present finite element model, the results obtained using FG flat panel model is compared with the published literature. The non-dimensional mid-point deflection $\bar{w} = \frac{w}{h}$ of square simply supported FG flat panel (a/h =5) are computed for five different power-law indices (n=0, 0.5,1,2, ∞) and tabulated in Table. It is observed from the results that convergence satisfies at a (16 x 16) mesh and the differences between present and published results are negligible.

Table 2: Convergence study of non-dimensional mid-point deflection of simply supported FG (Al_2O_3/ZrO_2) flat panel with $a/b = 1$ and $a/h = 5$)

n	Mesh size							Ref.[4]
	6x6	8x8	10x10	12x12	14x14	16x16	18x18	
Ceramic	0.024875	0.024855	0.024845	0.02484	0.024835	0.024835	0.024835	0.0247
0.5	0.031245	0.031215	0.0312	0.031195	0.03119	0.031185	0.03118	0.0313
1	0.03459	0.034555	0.03454	0.03453	0.03452	0.034515	0.034515	0.0351
2	0.037955	0.03792	0.0379	0.03789	0.03788	0.037875	0.03787	0.0388
Metal	0.05366	0.053615	0.053595	0.053585	0.053575	0.05357	0.05357	0.0534

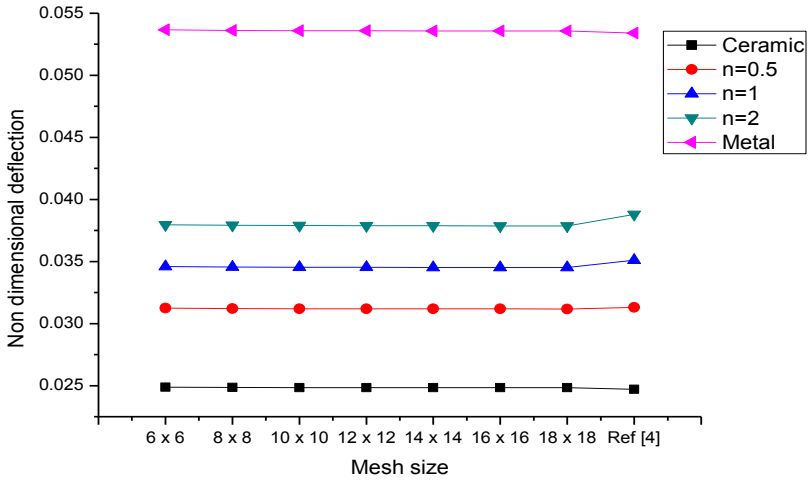

Figure 5: Variation of non-dimensional mid-point deflection with different mesh size in ANSYS SHELL 181 model for simply supported FGM plate

5.3 Numerical results:

In this section some new problems have been solved and new data, graphs are given for different parameters and responses are discusses. The variations of non-dimensional mid-point deflection of FG plate for simply supported boundary condition (SSSS) with different mess size in ANSYS SHELL 181 element are plotted in figure 6. The results are obtained using other geometric properties i.e., thickness ratio, aspect ratio for five fraction indices (n = 0, 0.5,1,2 and ∞). And also there are results for different material properties and different mesh size in ANSYS. Different material properties of FGM plates are given in table 1.

Graphs varying mesh size, thickness ratio and aspect ratio are plotted for aluminium/ zirconia, aluminium/ alumina, silicon nitride/stainless steel respectively. And also graphs are plotted for different boundary conditions for aluminium, zirconia FGM plates. Figure 7 and figure 8 shows the variation of thickness ratio and aspect ratio and central deflection varied. Figure 9-12 shows the central deflection varied under different boundary conditions for aluminium/zirconia plate. Figure 13-15 shows the behaviour of mid-point deflection if mesh size, thickness ratio and aspect ratio varies respectively for aluminium/alumina plate. For aluminium/stainless steel flat panel, the same behaviours are studied and plotted in figure 16-18.

5.3.1 Aluminium/Zirconia plate:

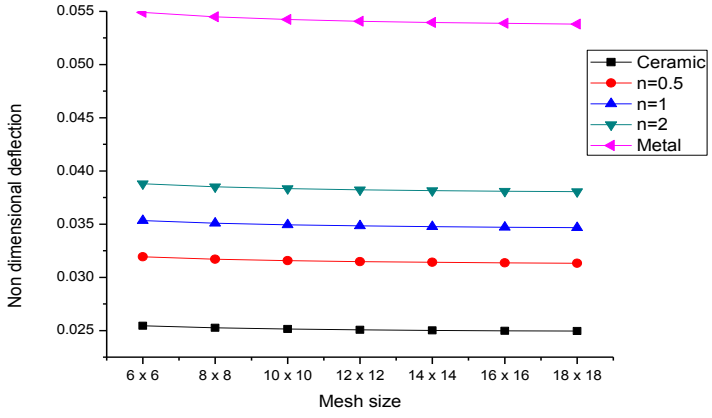

Figure 6: Variation of non-dimensional mid-point deflection with different mesh size in ANSYS SHELL 181 model for simply supported FGM plate

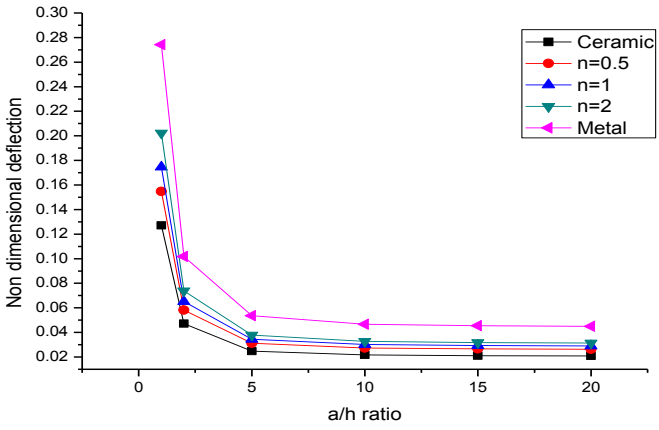

Figure 7: Variation of non-dimensional mid-point deflection with different thickness ratio (a/h ratio) in ANSYS SHELL 281 model for simply supported FGM plate

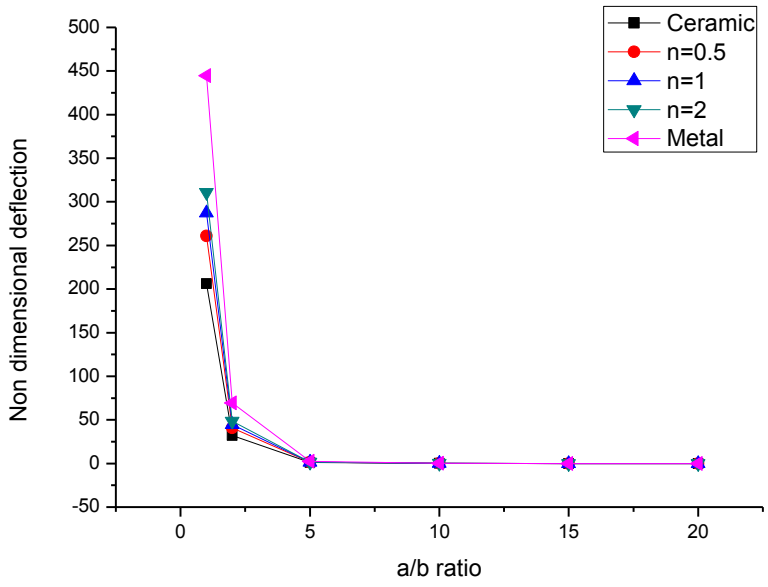

Figure 8: Variation of non-dimensional mid-point deflection with different aspect ratio (a/b ratio) in ANSYS SHELL 281 model for simply supported FGM plate

5.3.2 Different boundary conditions:

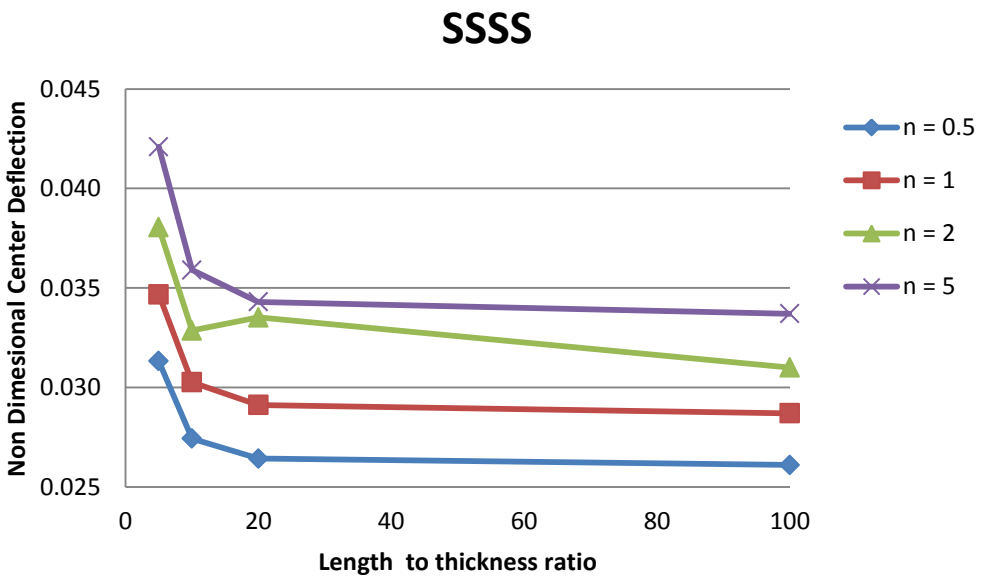

Figure 9: Non-dimensional deflection vs. Length to thickness ratio square FGM plate with simply supported (SSSS) boundary condition

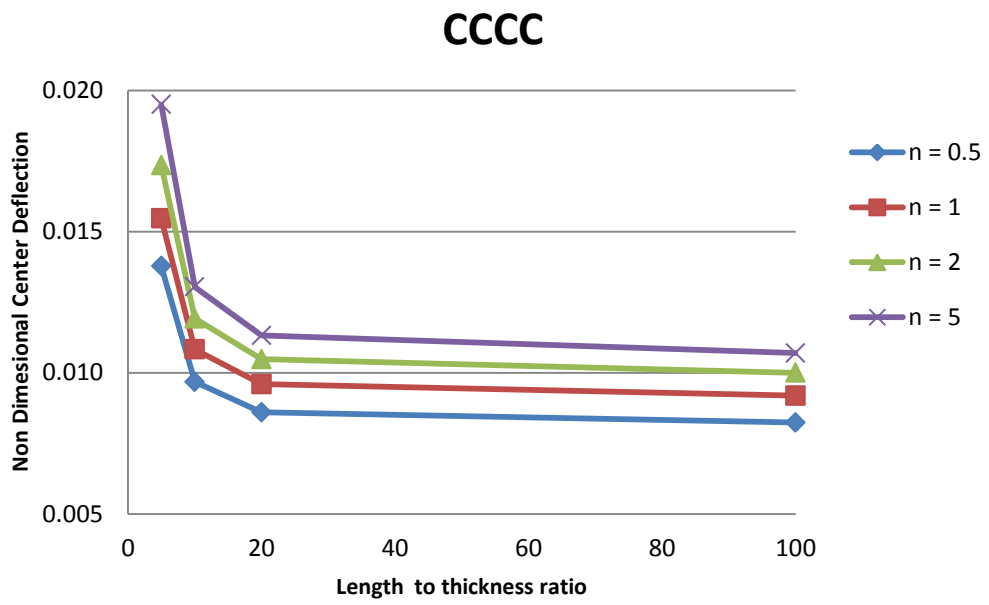

Figure 10: Non-dimensional deflection vs. Length to thickness ratio square FGM plate with clamped (CCCC) boundary condition

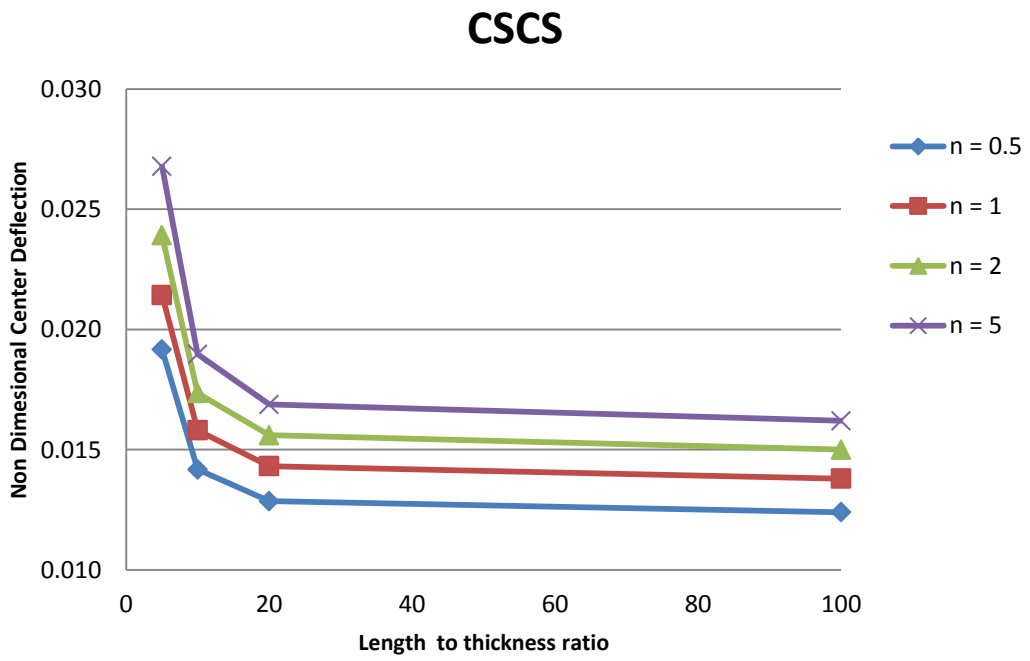

Figure 11: Non-dimensional deflection vs. Length to thickness ratio square FGM plate with clamped-simply supported (CSCS) boundary condition

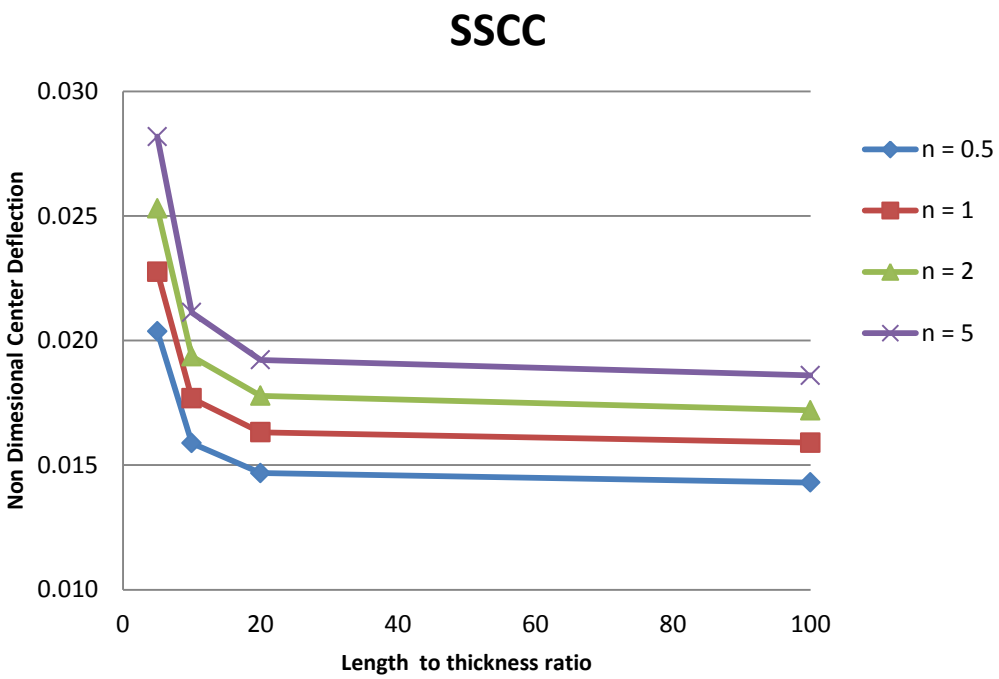

Figure 12: Non-dimensional deflection vs. Length to thickness ratio square FGM plate with clamped-simply supported (SSCC) boundary condition

5.3.3 Aluminium/Alumina plate:

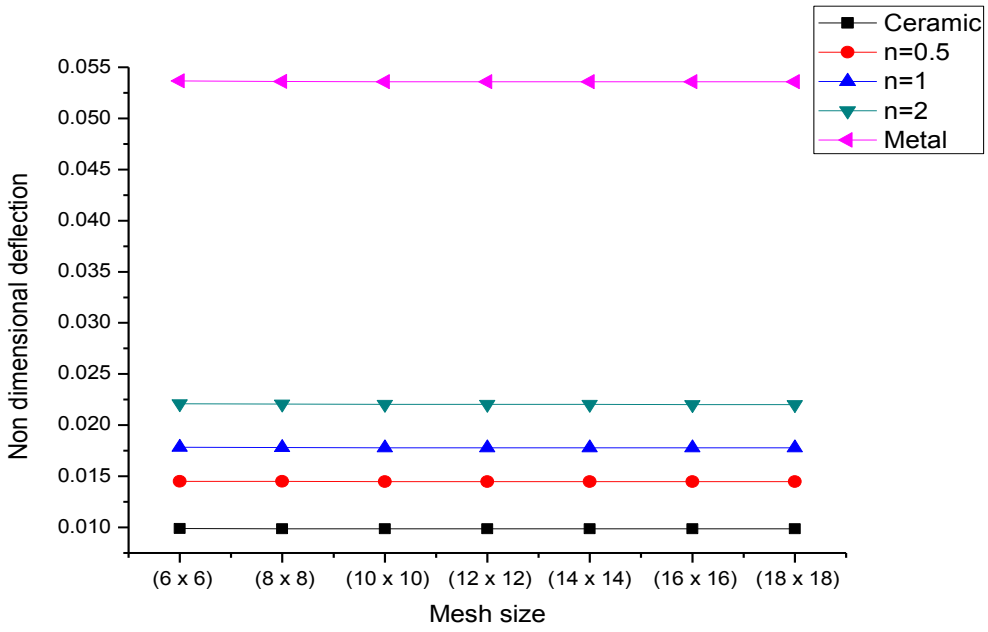

Figure 13: Variation of non-dimensional mid-point deflection with different mesh size in ANSYS SHELL 281 model for simply supported FGM plate

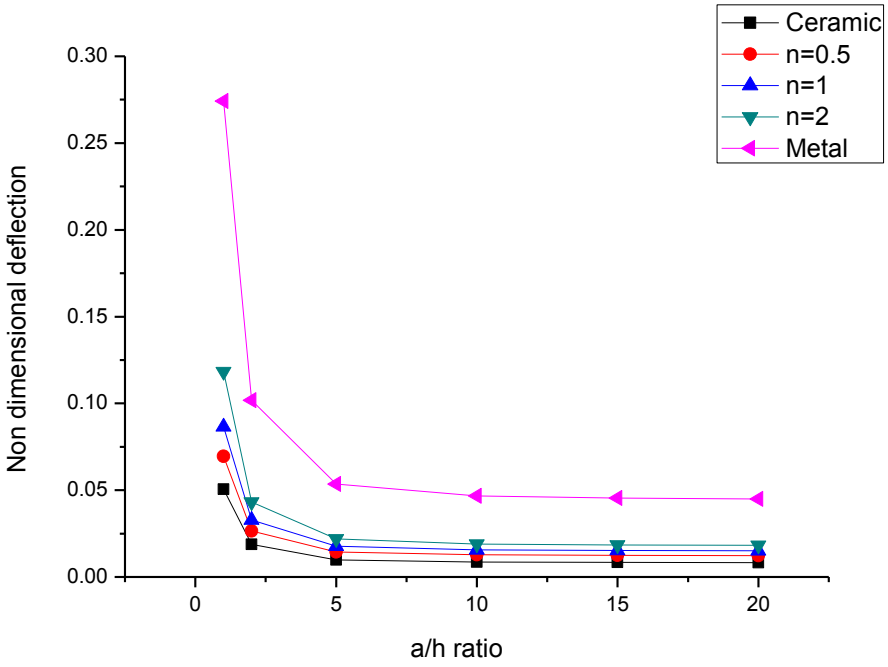

Figure 14: Variation of non-dimensional mid-point deflection with different thickness ratio (a/h ratio) in ANSYS SHELL 281 model for simply supported FGM plate

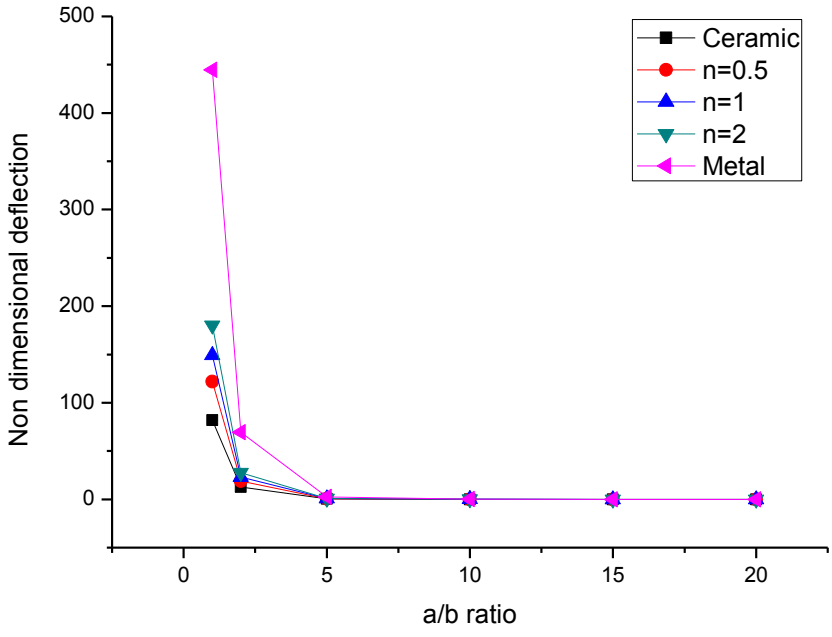

Figure 15: Variation of non-dimensional mid-point deflection with different aspect ratio (a/b ratio) in ANSYS SHELL 281 model for simply supported FGM plate

5.3.4 Silicon Nitride/Stainless steel plate:

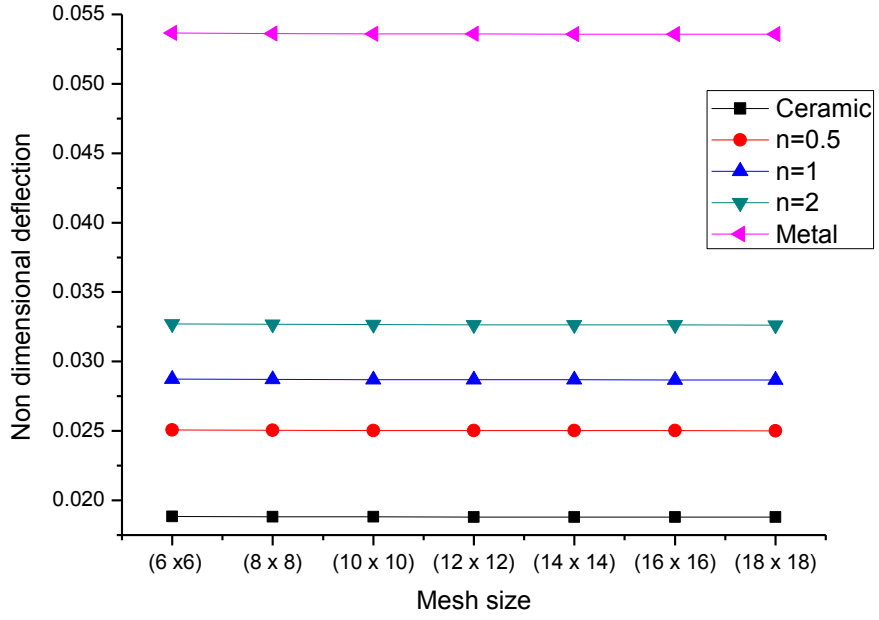

Figure 16: Variation of non-dimensional mid-point deflection with different mesh size in ANSYS SHELL 281 model for simply supported FGM plate

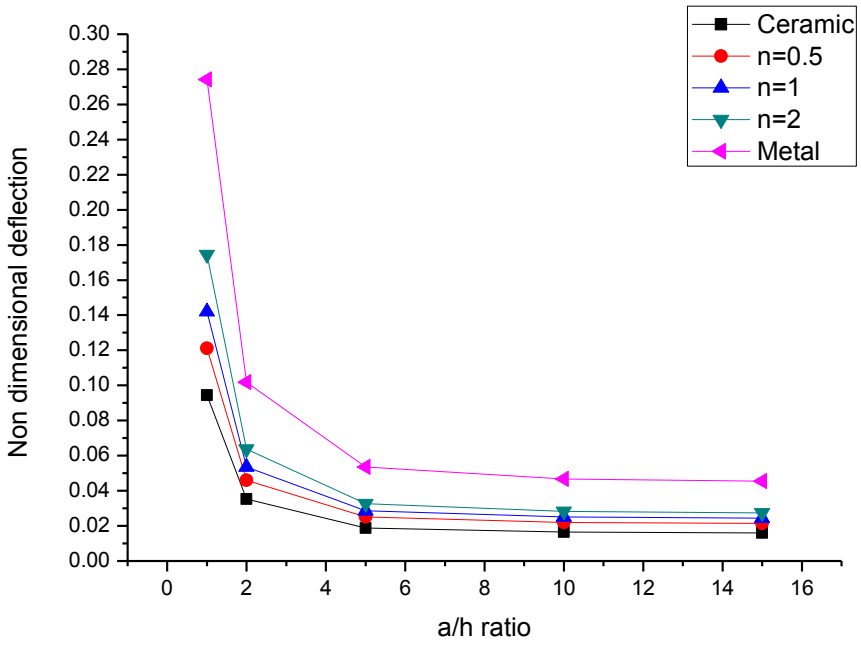

Figure 17: Variation of non-dimensional mid-point deflection with different thickness ratio (a/h ratio) in ANSYS SHELL 281 model for simply supported FGM plate

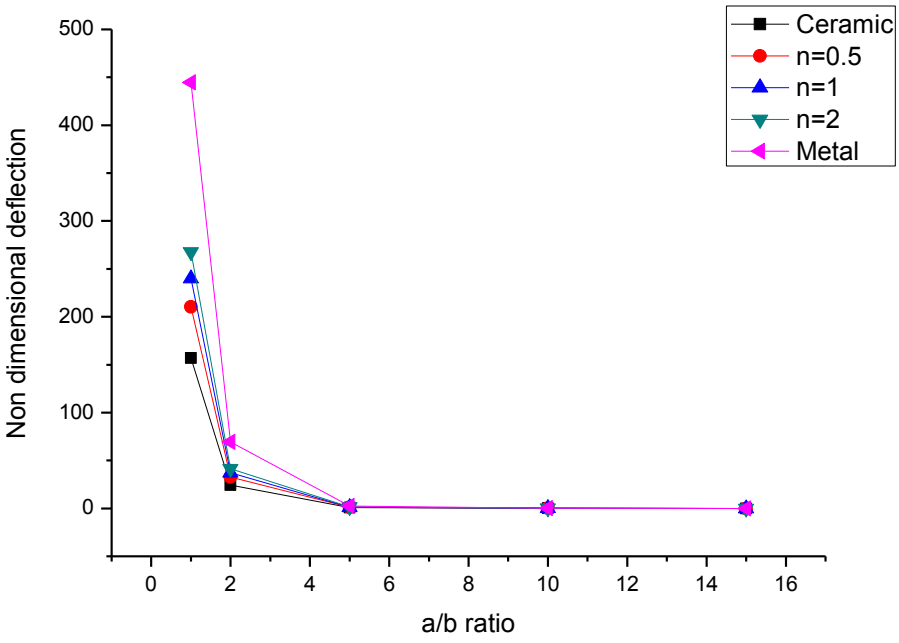

Figure 18: Variation of non-dimensional mid-point deflection with different aspect ratio (a/b ratio) in ANSYS SHELL 281 model for simply supported FGM plate

Chapter VI

Dynamic analysis

6.1 FG model (ANSYS)

Rectangular simply supported Aluminium/Zirconia FG flat panel has been developed in ANSYS13.0 platform. Time dependant step load has been taken for transient dynamic analysis. Step type loading has been taken in to consideration. From time 0 to 0.001s force is zero and from 0.001 to 0.002s force is 10kN. APDL code has been developed in ANSYS 13.0 for analysing the above panel.

6.2 Numerical results:

The analysis is carried out for different volume fraction indices (n=0, 1, 2, ∞). Dynamic behaviour of FG flat panel can be seen in figure 19-22. By time step of 0.0001s analysis has been performed and displacement has been plotted. . An enlarged view of dynamic response has been shown in figure 23 for ceramic flat panel.

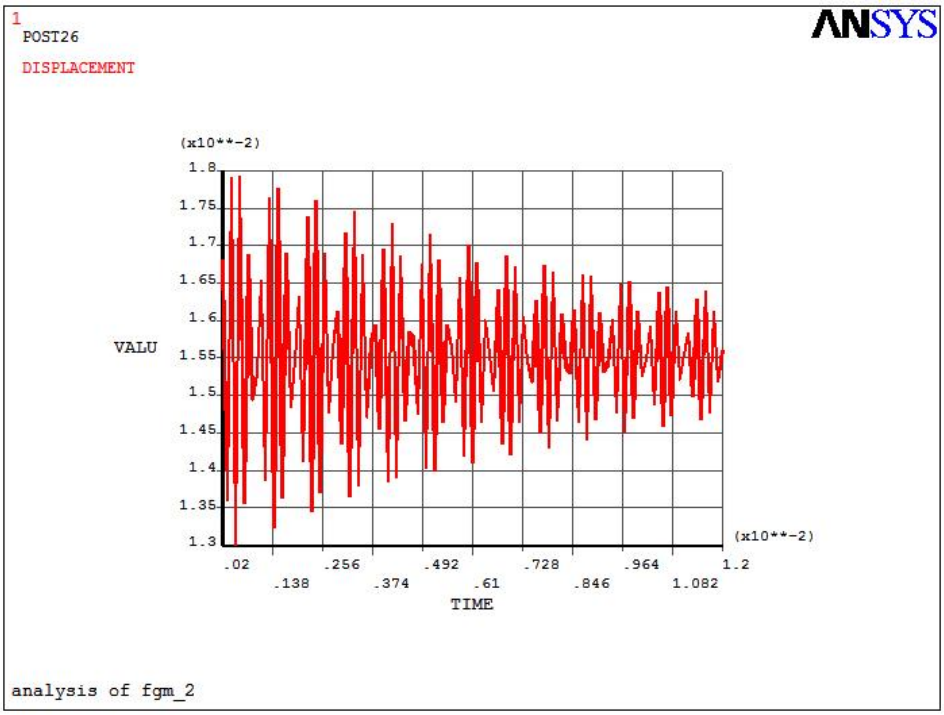

Figure 19: Deflection of mid-point of simply supported FG flat panel with n=0

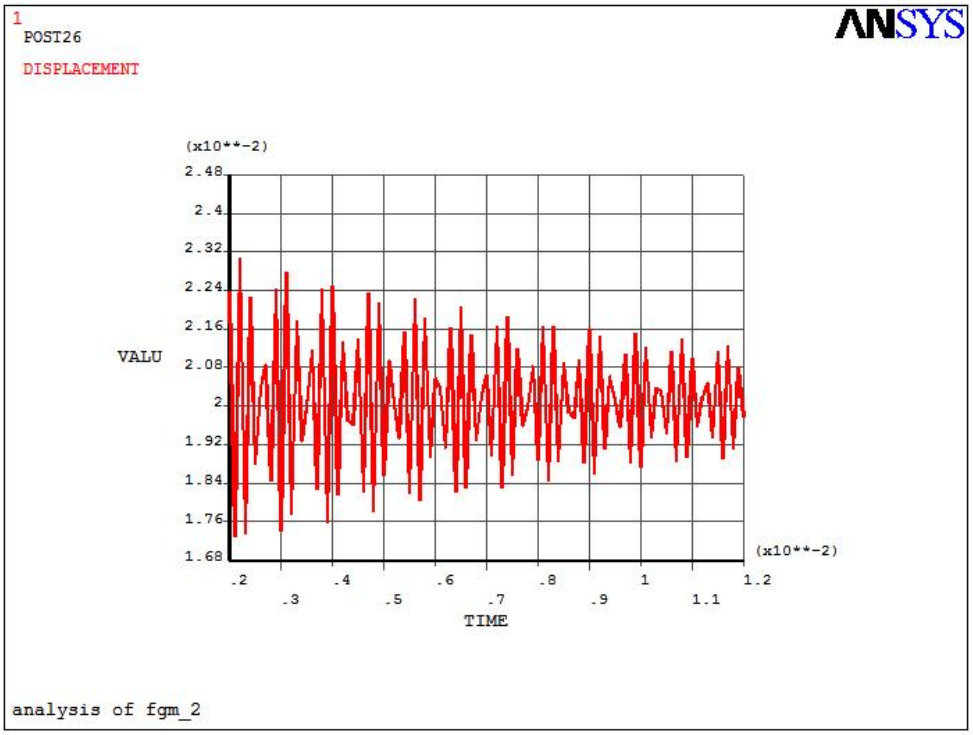

Figure 20: Deflection of mid-point of simply supported FG flat panel with n=1

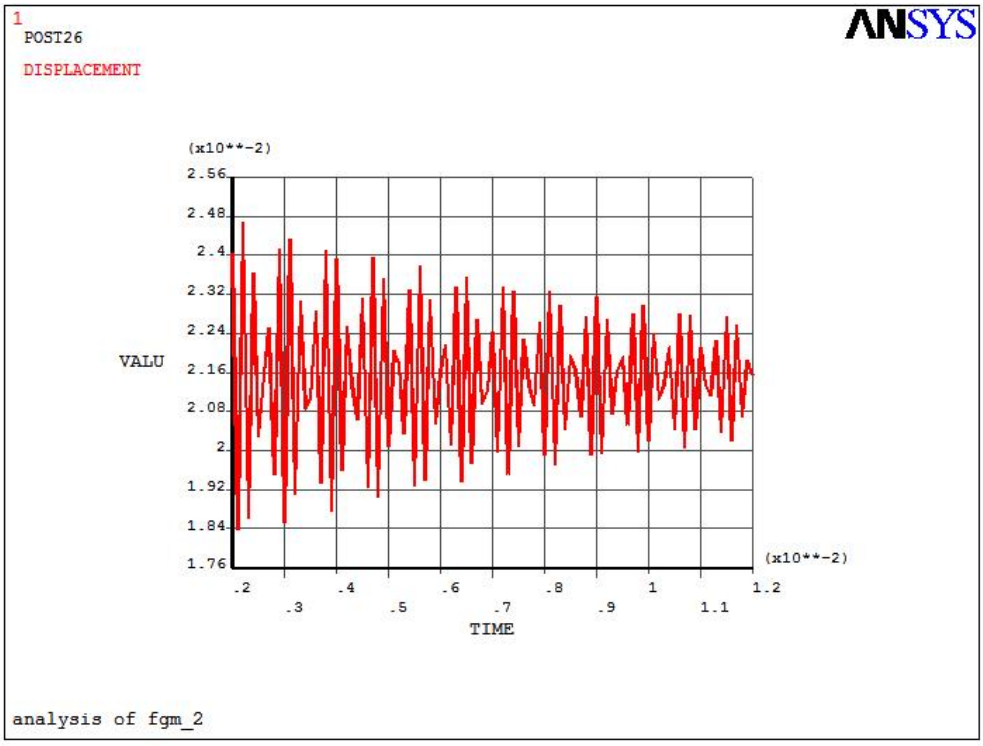

Figure 21: Deflection of mid-point of simply supported FG flat panel with n=2

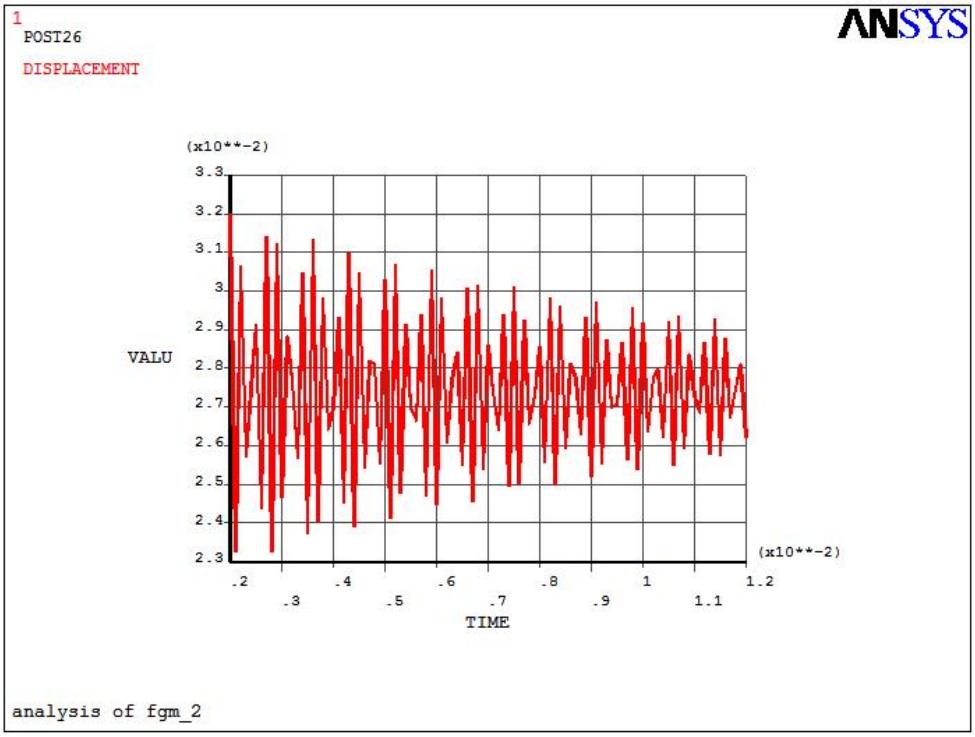

Figure 22: Deflection of mid-point of simply supported FG flat panel with n=∞

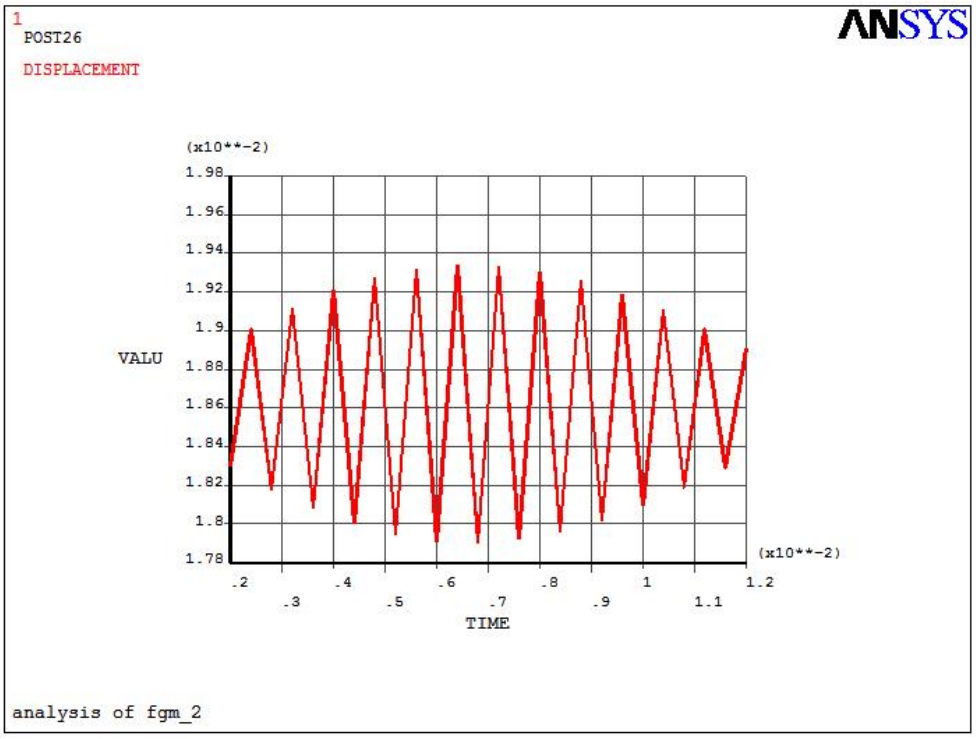

Figure 23: Deflection of mid-point of simply supported FG flat panel with n=0 in time interval of 0.0001 to 0.012s

Chapter VII

Conclusion

CHAPTER-7 CONCLUSION

7.1 Conclusion:

In this study, static and dynamic responses of FGM plates are analysed. The effective material properties of functionally graded materials for the plate structures are assumed to vary continuously through the plate thickness and are graded in the plate thickness direction according to a volume fraction power law distribution. Various boundary conditions have been considered to check the efficacy of ANSYS model. Convergence tests and comparison studies have been carried out with the commercially available software (ANSYS). An eight noded layered shell element (SHELL281) is used throughout the problem. The obtained results have illustrated a good agreement with those available in the literature for different volume fraction indices, thickness ratios, aspect ratios and different support conditions. The following points revealed the concluded remarks for thin to thick FGM plates are:

- For all the boundary conditions, the non-dimensional central deflection increases as the volume fraction index increases.
- For all the boundary conditions, the non-dimensional central deflection increases as the aspect ratio increases
- For all the boundary conditions, the non-dimensional central deflection increases as the thickness ratio increases
- For simply supported boundary condition vibration amplitude increases as the volume fraction index increases.

7.2 Future Scope of work

- Different geometric structures can be modelled such as cylindrical, spherical, conical, hyperboloid etc.
- Temperature dependent material property can be considered.
- Different type of analysis like buckling, post buckling, free vibration, forced vibration etc. can also be performed using the presented model.

REFERENCES

[1] Mohammad Talha, B.N. Singh, Static response and free vibration analysis of FGM plates using higher order shear deformation theory, Applied Mathematical Modelling 34 (2010) 3991–4011

[2] A.M.A. Neves et al. Bending of FGM plates by a sinusoidal plate formulation and collocation with radial basis functions. Mechanics Research Communications 38 (2011) 368– 371

[3] B. Sobhani Aragh, H. Hedayati. Static response and free vibration of two-dimensional functionally graded metal/ceramic open cylindrical shells under various boundary conditions. Acta Mech 223,(2012) 309–330

[4] A.J.M. Ferreira, R.C. Batra, C.M.C. Roque, L.F. Qian, P.A.L.S. Martins. Static analysis of functionally graded plates using third-order shear deformation theory and a meshless method. Composite Structures 69 (2005) 449–457

[5] J N Reddy. Mechanics of laminated composite: Plates and shells-Theory and analysis. Second edition. CRC press.2003

[6] Abrate S., Free vibration, buckling, and static deflections of functionally graded plates. Compos Sci Technol 2006;66:2383–94.

[7] A.M. Zenkour, Generalised shear deformation theory for bending analysis of functionally graded plates, Appl. Math. Model. 30 (2006) 67–84.

[8] A.J.M. Ferreira, R.C. Batra, C.M.C. Roque, L.F. Qian, P.A.L.S. Martins, Static analysis of functionally graded plates using third order shear deformation theory and a meshless method, Compos. Struct. 69 (2005) 449–457.

[9] Vel SS, Batra RC. Exact solutions for thermoelastic deformations of functionally graded thick rectangular plates. AIAA J 2002; 40(7):1421–33.

[10] Qian LF, Batra RC, Chen LM. Static and dynamic deformations of thick functionally graded elastic plate by using higher-order shear and normal deformable plate theory and meshless local Petrov–Galerkin method.Composites Part B 2004;35:685–97.

[11] Ramirez F, Heyliger PR, Pan E. Static analysis of functionally graded elastic anisotropic plates using a discrete layer approach. Composites Part B 2006; 37:10–20

[12] Zenkour AM. Benchmark trigonometric and 3-D elasticity solutions for an exponentially graded thick rectangular plate. Arch Appl Mech 2007; 77:197–214.

[13] Bhangale RK, Ganesan N. Static analysis of simply supported functionally graded and layered magneto-electro-elastic plates. Int J Solids Struct 2006; 43:3230–53.

[14] Aghdam MM, Bigdelli K, Shahmansouri N. A semi-analytical solution for bending of moderately thick curved functionally graded panels. Mech Adv Mater Struct 2010;17:320–7.

[15] Neves AMA, Ferreira AJM, Carrera E, Roque CMC, Cinefra M, Jorge RMN, et al. A quasi-3D sinusoidal shear deformation theory for the static and free vibration analysis of functionally graded plates. Composites Part B 2012; 43:711–25.

[16] Talha M, Singh BN. Static response and free vibration analysis of FGM plates using higher order shear deformation theory. Appl Math Model 2010; 34:3991–4011.

[17] Hoang VT, Nguyen DD. Nonlinear analysis of stability for functionally graded plates under mechanical and thermal loads. Compos Struct. 2010; 92:1184–91.

[18] Yang J., Shen Hui-Shen, Dynamic response of initially stressed functionally graded rectangular thin plates, composite structures 54 (2001) 497-508.

[19] Yang J., Shen H. S.,Vibration characteristics and transient response of shear-deformable functionally graded plates in thermal environments, Journal of Sound and Vibration (2002) 255(3), 579-602.

[20] Yang J., Liew K. M., Kitipornchai S., Dynamic stability of laminated FGM plates based on higher-order shear deformation theory, Computational Mechanics 33 (2004) 305–315.

[21] Kim Young-Wann, Temperature dependent vibration analysis of functionally graded rectangular plates, Journal of Sound and Vibration 284 (2005) 531–549.

[22] Lanhe Wu, Hongjun Wang, Daobin Wang, Dynamic stability analysis of FGM plates by the moving least squares differential quadrature method, Composite Structures 77 (2007) 383–394.

[23] Ansari R., Darvizeh M., Prediction of dynamic behaviour of FGM shells under arbitrary boundary conditions, Composite Structures 85 (2008) 284–292.

[24] Behjat B., Salehi M., Armin A., Sadighi M., Abbasi M.,Static and dynamic analysis of functionally graded piezoelectric plates under mechanical and electrical loading, Scientia Iranica B (2011) 18 (4), 986–994.

[25] Sladek J, Sladek V, Hellmich CH, Eberhardsteiner J. Analysis of thick functionally graded plates by local integral equation. Commun Numer Meth Eng 2007;23:733–54
.
[26] Wen PH, Sladek J, Sladek V. Three-dimensional analysis of functionally graded plates. Int J Numer Meth Eng 2011;87(10):923–42.

[27] Shariyat M. Vibration and dynamic buckling control of imperfect hybrid FGM plates with temperature-dependent material properties subjected to thermo-electro-mechanical loading conditions. Compos Struct 2009;88:240–52.

Appendix-A

$$u(x,y,z) = u^0(x,y) + z\theta_x(x,y)$$
$$v(x,y,z) = v^0(x,y) + z\theta_y(x,y)$$
$$w(x,y,z) = w^0(x,y) + z\theta_z(x,y)$$

$$\varepsilon_{xx} = \frac{\partial u_0}{\partial x} + z\frac{\partial \theta_x}{\partial x} + \frac{w_0}{R_x} + z\frac{\theta_z}{R_x} = (\frac{\partial u_0}{\partial x} + \frac{w_0}{R_x}) + z(\frac{\partial \theta_x}{\partial x} + \frac{\theta_z}{R_x})$$
$$\varepsilon_{yy} = \frac{\partial u_0}{\partial x} + z\frac{\partial \theta_y}{\partial y} + \frac{w_0}{R_y} + z\frac{\theta_z}{R_y} = (\frac{\partial v_0}{\partial y} + \frac{w_0}{R_y}) + z(\frac{\partial \theta_y}{\partial y} + \frac{\theta_z}{R_y})$$
$$\varepsilon_{zz} = \theta_z$$
$$\gamma_{yz} = \theta_y + \frac{\partial w_0}{\partial y} + z\frac{\partial \theta_z}{\partial y} - \frac{v_0}{R_y} - z\frac{\theta_y}{R_y} = (\theta_y + \frac{\partial w_0}{\partial y} - \frac{v_0}{R_y}) + z(\frac{\partial \theta_z}{\partial y} - \frac{\theta_y}{R_y})$$
$$\gamma_{xz} = \theta_x + \frac{\partial w_0}{\partial y} + z\frac{\partial \theta_z}{\partial y} - \frac{u_0}{R_x} - z\frac{\theta_x}{R_x} = (\theta_x + \frac{\partial w_0}{\partial y} - \frac{u_0}{R_x}) + z(\frac{\partial \theta_z}{\partial y} - \frac{\theta_x}{R_x})$$
$$\gamma_{xy} = \frac{\partial y}{\partial u_0} + z\frac{\partial \theta_x}{\partial y} + \frac{\partial v_0}{\partial x} + z\frac{\partial \theta_y}{\partial x} + \frac{2w_0}{R_{xy}} + z\frac{\theta_z}{R_{xy}} = (\frac{\partial y}{\partial u_0} + \frac{\partial v_0}{\partial x} + \frac{2w_0}{R_{xy}}) + z(\frac{\partial \theta_x}{\partial y} + \frac{\partial \theta_y}{\partial x} + \frac{\theta_z}{R_{xy}})$$

$$\varepsilon_l = \begin{bmatrix} 1 & 0 & 0 & 0 & 0 & 0 & z & 0 & 0 & 0 & 0 & 0 \\ 0 & 1 & 0 & 0 & 0 & 0 & 0 & z & 0 & 0 & 0 & 0 \\ 0 & 0 & 1 & 0 & 0 & 0 & 0 & 0 & z & 0 & 0 & 0 \\ 0 & 0 & 0 & 1 & 0 & 0 & 0 & 0 & 0 & z & 0 & 0 \\ 0 & 0 & 0 & 0 & 1 & 0 & 0 & 0 & 0 & 0 & z & 0 \\ 0 & 0 & 0 & 0 & 0 & 1 & 0 & 0 & 0 & 0 & 0 & z \end{bmatrix} \begin{bmatrix} \varepsilon_x^0 \\ \varepsilon_y^0 \\ \varepsilon_z^0 \\ \varepsilon_{yz}^0 \\ \varepsilon_{xz}^0 \\ \varepsilon_{xy}^0 \\ k_x' \\ k_y' \\ k_z' \\ k_{yz}' \\ k_{xz}' \\ k_{xy}' \end{bmatrix}$$

$$\begin{bmatrix} \varepsilon_x^0 \\ \varepsilon_y^0 \\ \varepsilon_z^0 \\ \varepsilon_{yz}^0 \\ \varepsilon_{xz}^0 \\ \varepsilon_{xy}^0 \\ k_x^{'} \\ k_y^{'} \\ k_z^{'} \\ k_{yz}^{'} \\ k_{xz}^{'} \\ k_{xy}^{'} \end{bmatrix} = \begin{bmatrix} \frac{\partial}{\partial x} & 0 & \frac{1}{R_x} & 0 & 0 & 0 \\ 0 & \frac{\partial}{\partial y} & \frac{1}{R_y} & 0 & 0 & 0 \\ 0 & 0 & 0 & 0 & 0 & 1 \\ 0 & -\frac{1}{R_y} & \frac{\partial}{\partial y} & 0 & 1 & 0 \\ -\frac{1}{R_x} & 0 & \frac{\partial}{\partial y} & 1 & 0 & 0 \\ \frac{\partial}{\partial y} & \frac{\partial}{\partial x} & \frac{2}{R_{xy}} & 0 & 0 & 0 \\ 0 & 0 & 0 & \frac{\partial}{\partial x} & 0 & \frac{1}{R_x} \\ 0 & 0 & 0 & 0 & \frac{\partial}{\partial y} & \frac{1}{R_y} \\ 0 & 0 & 0 & 0 & 0 & 0 \\ 0 & 0 & 0 & 0 & -\frac{1}{R_y} & \frac{\partial}{\partial y} \\ 0 & 0 & 0 & -\frac{1}{R_x} & 0 & \frac{\partial}{\partial y} \\ 0 & 0 & 0 & \frac{\partial}{\partial y} & \frac{\partial}{\partial x} & \frac{1}{R_{xy}} \end{bmatrix} \cdot \begin{bmatrix} u_0 \\ v_0 \\ w_0 \\ \theta_x \\ \theta_y \\ \theta_z \end{bmatrix}$$

$$\overline{Q} = \begin{bmatrix} Q_{11} & Q_{12} & Q_{13} & 0 & 0 & 0 & zQ_{11} & zQ_{12} & zQ_{13} & 0 & 0 & 0 \\ Q_{21} & Q_{22} & Q_{23} & 0 & 0 & 0 & zQ_{21} & zQ_{22} & zQ_{23} & 0 & 0 & 0 \\ Q_{31} & Q_{32} & Q_{33} & 0 & 0 & 0 & zQ_{31} & zQ_{32} & zQ_{33} & 0 & 0 & 0 \\ 0 & 0 & 0 & Q_{44} & 0 & 0 & 0 & 0 & 0 & zQ_{44} & 0 & 0 \\ 0 & 0 & 0 & 0 & Q_{55} & 0 & 0 & 0 & 0 & 0 & zQ_{55} & 0 \\ 0 & 0 & 0 & 0 & 0 & Q_{66} & 0 & 0 & 0 & 0 & 0 & zQ_{66} \\ zQ_{11} & zQ_{12} & zQ_{13} & 0 & 0 & 0 & z^2Q_{11} & z^2Q_{12} & z^2Q_{13} & 0 & 0 & 0 \\ zQ_{21} & zQ_{22} & zQ_{23} & 0 & 0 & 0 & z^2Q_{21} & zQ_{22}^2 & z^2Q_{23} & 0 & 0 & 0 \\ zQ_{31} & zQ_{32} & zQ_{33} & 0 & 0 & 0 & z^2Q_{31} & z^2Q_{32} & z^2Q_{33} & 0 & 0 & 0 \\ 0 & 0 & 0 & zQ_{44} & 0 & 0 & 0 & 0 & 0 & z^2Q_{44} & 0 & 0 \\ 0 & 0 & 0 & 0 & zQ_{55} & 0 & 0 & 0 & 0 & 0 & z^2Q_{55} & 0 \\ 0 & 0 & 0 & 0 & 0 & zQ_{66} & 0 & 0 & 0 & 0 & 0 & z^2Q_{66} \end{bmatrix}$$